

# DRAMA+: Disaster Management With Mitigation Awareness for Translucent Elastic Optical Networks

Rujia Zou<sup>1</sup>, *Graduate Student Member, IEEE*, Hiroshi Hasegawa, *Senior Member, IEEE*,  
Masahiko Jinno<sup>1</sup>, *Fellow, IEEE*, and Suresh Subramaniam<sup>1</sup>, *Fellow, IEEE*

**Abstract**—Elastic optical networks (EONs) have emerged as attractive candidates to satisfy the dramatic growth of demand in 5G and cloud applications. EONs promise to provide high spectrum utilization due to flexibility in resource assignment. In translucent EONs, the spectrum efficiency can be further improved by deploying regenerators. Because of their extremely high flexibility, developing efficient mechanisms and strategies to ensure the survivability of translucent EONs is a challenging problem. In this paper, we consider disaster mitigation in translucent EONs. We propose a new approach to disaster management by introducing the concept of *mitigation zone*, which identifies a region surrounding the disaster zone wherein lightpaths may be reconfigured with degraded service (with a penalty) in order to improve overall performance. We formulate an integer linear program (ILP) to minimize the penalty due to service degradation after a disaster, and present a heuristic algorithm named Disaster Management Algorithm with Mitigation Awareness and 3R regenerators (DRAMA+). Simulation results demonstrate that the proposed algorithms have a better performance in terms of total penalty and blocking ratio than conventional disaster recovery algorithms.

**Index Terms**—Survivability, disaster management, mitigation, degraded service.

## I. INTRODUCTION

ELASTIC optical networks (EONs) are considered as attractive candidates for satisfying the dramatic growth of network traffic because of their flexibility in resource allocation and spectrum assignment [1]. EONs use a flexible frequency grid of 6.25 GHz spacing and reduce the bandwidth allocation level to Frequency Slot (FS), which is 12.5 GHz wide [2], compared to traditional fixed-grid wavelength division multiplexing (WDM) that uses a grid of 25 or 50 GHz and allocates whole wavelengths to lightpaths. Further, the development of transceivers that support

Manuscript received 20 November 2021; revised 30 April 2022; accepted 24 June 2022. Date of publication 8 July 2022; date of current version 12 October 2022. This work was supported in part by NSF grant CNS-1818858. The associate editor coordinating the review of this article and approving it for publication was M. Tornatore. (Corresponding author: Rujia Zou.)

Rujia Zou and Suresh Subramaniam are with the Department of Electrical and Computer Engineering, The George Washington University, Washington, DC 20052 USA (e-mail: rjzou@gwu.edu; suresh@gwu.edu).

Hiroshi Hasegawa is with the Department of Electrical Engineering and Computer Science, Nagoya University, Nagoya 464-8603, Japan (e-mail: hasegawa@nuee.nagoya-u.ac.jp).

Masahiko Jinno is with the Department of Electronics and Information Engineering, Kagawa University, Takamatsu 760-0016, Japan (e-mail: jinno@eng.kagawa-u.ac.jp).

Digital Object Identifier 10.1109/TNSM.2022.3189362

multiple modulation formats has made it possible to allocate spectrum to services as needed with the highest spectral efficiency [3]. Thus, the resource allocation issue has evolved from the routing and wavelength assignment problem in traditional WDM networks into the routing, modulation, and spectrum assignment problem with spectrum continuity and spectrum contiguity in EONs [4], [5]. With the deployment of 3R-regenerators (devices with re-amplification, reshaping, and re-timing function), translucent EONs achieve high spectrum utilization due to the increase of reach and more flexible spectrum assignment [6]–[8].

Survivability is an important aspect of optical networks. Survivability strategies can be generally divided into either protection or restoration [9]. Protection approaches aim to reserve backup resources before a network failure happens, while spare resources for recovery are identified after a failure happens in the case of restoration [10], [11].

Disaster recovery is a special case of survivability [12]. Many survivability approaches are typically designed for small-scale failures such as a single failure or the failure of a small set of nodes and/or links [13]. However, in disaster scenarios, such as earthquakes and hurricanes, the network infrastructure may suffer widespread damage [11]. As the probability of disasters is rather small, protection is not a cost-effective strategy as it may need significant backup resources that are unlikely to ever be needed. In this case, dynamic restoration is a better solution due to lower redundancy [14], [15].

We note that while disaster management in optical networks has been investigated for a number of years, its application to EONs is relatively sparse. Further, to our knowledge, ours is the first work to consider degraded service recovery for translucent EONs. In translucent EONs, how to utilize the availability of 3R-regenerators for better recovery after a disaster happens is a challenge. In this paper, we propose a new approach to disaster recovery; an earlier version of which was first presented in [11]. Our approach is based on the intuition that services that are far away from the disaster zone should not be affected much (or at all) during the recovery process.

To this end, we introduced the idea of *mitigation zone*, which is an area surrounding the disaster zone, in [11]. In [11], we proposed that lightpaths inside the mitigation zone may be recovered with degraded service (at the cost of a penalty), whereas those outside the zone should not be degraded at all.

While we observed significant performance improvement over traditional approaches that did not consider degraded recovery or differentiate between various lightpaths, we also noted that the surviving network may be very resource-constrained causing many lightpaths outside the mitigation zone to not be recovered at all.

This paper extends and improves upon our earlier work [11] in several ways. First, we make the recovery process more flexible by allowing all lightpaths to be recovered with degraded service, but those outside the mitigation zone would suffer a larger penalty than those inside the zone. Second, we consider translucent EONs in this work, thus generalizing the recovery algorithm in [11] that was restricted to transparent networks. Third, an Integer Linear Program (ILP) is formulated to minimize the penalty for small problem instances, and an enhanced heuristic algorithm, named Disaster Recovery Algorithm with Mitigation Awareness (DRAMA+), is designed for more realistic problem instances. Fourth, multiple penalty functions are proposed to fairly measure the cost of recovery with degradation and fully test the heuristic algorithm. Finally, we present extensive simulation results to show that our proposed approach has better performance than conventional recovery methods.

The paper is organized as follows. Related work is summarized in Section II. The disaster recovery problem and penalty functions are presented in Section III. The ILP is formulated in Section IV. This is followed by our heuristic algorithm DRAMA+ in Section V. Extensive simulation results are presented and analyzed in Section VI, and the paper is concluded in Section VII.

## II. RELATED WORK

Because of the drastic impact of failures, survivability in general and disaster recovery in particular have been studied extensively. Here, we briefly review the related work on survivability and disaster recovery in optical networks. Survivability strategies can be generally divided into protection and restoration. In protection, backup paths of the traffic are determined in advance for planned failure scenarios. Protection and restoration from small-scale failures in optical networks have been researched extensively over decades [16]–[19].

However, protection is not suitable for disaster recovery due to its low efficiency. Moreover, recovery strategies for small-scale failures may not be directly applicable for disaster recovery. Disaster recovery in optical networks has been explored much less, and we summarize the existing literature below.

In [20], a joint progressive recovery algorithm for a WDM network with datacenters is proposed to recover the network nodes and datacenters after large-scale disasters. In [21], disaster management is formulated as a repairman scheduling problem. This work focuses on how to physically repair the damaged network infrastructure. A mixed integer linear program (MILP) and three heuristic algorithms are proposed to find the repair schedules and restoration order of failed components. These two papers investigate the disaster management

problem in terms of network repair as opposed to the recovery of lightpaths.

In [22], the disaster survivability problem is addressed through an architecture of a bandwidth-variable wavelength cross-connect. In [23], the authors propose a node architecture with optical packet/circuit hybrid switching to mitigate congestion after disaster. A multi-vendor interconnection and a hierarchical addressing technique are presented for quick recovery. That paper focuses on the hardware design for disaster management.

The following papers focus directly on the recovery of the network after a disaster. In [12], a network component recovery algorithm is proposed to maximize the routed traffic demand after disaster. An MILP and a heuristic algorithm are designed. In [14], a heuristic traffic recovery algorithm is proposed with genetic operator for EONs, where the genetic operator is used to optimize the serving order for failed services. The feasible ordering configurations are generated iteratively and solutions that increase the network recovery capability are retained. In [15], a capacity-constrained maximally spatial disjoint lightpath algorithm is proposed for EONs. This algorithm computes alternate least loaded lightpaths for disrupted primary lightpaths using capacity-constrained shortest lightpaths. In [24], the rerouting and traffic flooding problems after disaster in a WDM network are investigated. In [25], an efficient algorithm based on dynamic programming is proposed to add new links and recover from the failure. However, this work is for general networks and does not consider specific characteristics of EONs. In [26], a probabilistic risk model to analyze the loss/penalty is presented first. Later, a proactive solution for disaster protection is proposed, while a reactive solution is also designed, where disrupted connections and connections under the risk of correlated cascading failures are reprovisioned. However, that work is designed for WDM networks without consideration of EONs. In [27], a network protection approach against disasters is designed for WDM optical networks with datacenters. That work allows for recovery with degraded service, but the degradation level is fixed.

## III. MOTIVATION AND PROBLEM STATEMENT

### A. Motivation

When a disaster happens, a part of the network is disabled, thereby disrupting some traffic by either damaging the source or destination of the traffic or by damaging one or more components along the traffic's route. The former traffic is not recoverable of course, but the latter traffic may be recovered by re-assigning resources on the surviving network, which is capacity-limited due to several component failures. In this scenario, it may be more desirable to recover more traffic at a reduced level of service as opposed to recover some traffic at their pre-disaster level of service and completely drop the other traffic.

The idea of providing degraded service through grooming has been explored before for WDM networks in [28], [29]. While the concept of degraded service recovery has merit, we also note that the network operator must have control over

which lightpaths can be degraded and to what extent. Intuition would suggest that degraded service may be more acceptable physically near the disaster than far away from the disaster. As an analogy, it is usual for a government to provide supply assistance to a disaster area from nearby areas than from farther areas. Accordingly, we introduced the concept of *mitigation zone* in [11]. The mitigation zone is an area surrounding the disaster zone within which any service<sup>1</sup> may be re-assigned resources and degraded in the disaster recovery process with a relatively low penalty. Services outside the mitigation zone, on the other hand, may be degraded during recovery but this incurs a higher penalty. The network operator may adjust the mitigation zone as needed. For example, if the mitigation zone is the *same* as the disaster zone, then there is a steep penalty for degrading *any* service. On the other hand, if the mitigation zone is the entire network (excluding the disaster zone), then all services may be degraded without any distinction in incurred penalty, giving the network operator the most flexibility in recovery. Depending on how service level agreements (SLAs) are structured, the operator might define a mitigation zone which is in between these two extremes. We note that our approach is simply one way of selecting differential degraded service candidates; alternatively, one may simply have a list of services, each of which has a specified penalty for each degradation level. Our work can be easily adapted to such a situation.

### B. The Disaster Recovery Problem

1) *Network and Traffic Model*: The disaster recovery problem is defined as follows. Consider a network  $G(N, E)$  with 3R-regenerators, where  $N$  denotes the node set and  $E$  denotes the link set. On each link  $e$ , there is a pair of oppositely-directed fibers. We assume that, before the disaster happens, a set of LPs  $L$  exists in the network. Each LP is denoted as  $l(s, d, w)$ , where  $s$  represents the source node,  $d$  represents the destination node, and  $w$  represents the lightpath (LP) data rate. Assume there are several modulation formats with different spectrum efficiencies and distance limitations. Given the locations of 3R-regenerators, we assume that the 3R-regenerators at a node are available for all LPs passing through that node. We assume that a 3R-regenerator can be used to perform spectrum conversion, as well as extend the LP transmission distance and/or increase the modulation level.

Consider a circular *disaster zone*  $D(C_d, R_d)$ , where  $C_d$  represents the center and  $R_d$  represents the radius. We assume that any node that lies in the disaster zone and any link with either end node in the disaster zone is failed due to the disaster. If either source node or destination node is failed after the disaster, the LP is considered as *unrecoverable*. Further, if there is no possible path from an LP's source node to its destination node, then the LP is *unrecoverable* as well.

The *mitigation zone*  $M(C_m, R_m)$  is formed as the annulus bounded by the circular region with the same center as disaster  $C_m = C_d$  and radius  $R_d + R_m$ . The network excluding the disaster and the mitigation zones is denoted as  $U$ .

<sup>1</sup>We use the terms service, traffic, and lightpath interchangeably in this paper.

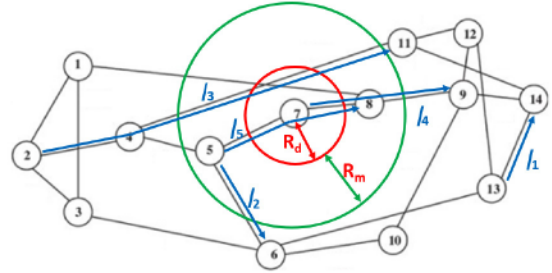


Fig. 1. Examples of LPs inside and outside the disaster and mitigation zones.

The network is thus covered by three disjoint zones:  $D$ ,  $M$ , and  $U$ . Every LP  $l \in L$  is considered to be in one of the three zones, determined by where their source/destination nodes lie. If either the source node or the destination node lies in  $D$ , then the LP is regarded as  $l \in D$  and is *unrecoverable*. For all recoverable LPs, if either source or destination node lies within  $M$ , then we say  $l \in M$ ; else,  $l \in U$ .

We explain these ideas with an example in Fig. 1. Here, the center of the disaster and mitigation zones is node 7. The disaster zone is shown as the red circle, while the mitigation zone is shown as the green circle. Node 7, links 1-8, 4-11, 5-7 and 7-8 are disabled by the disaster, while nodes 5 and 8 are inside the mitigation zone. Based on affected/unaffected situation and the three different zones, all the LPs can be divided into 4 types and managed in different ways:

- If the LP is *unrecoverable*, the LP will be dropped without recovery attempt. This case is shown as  $l_4$ .
- If the LP (in  $M$  or  $U$ ) is affected by the disaster, the LP is recovered with a new path and FSs with possibly degraded data rate. This case is shown as  $l_3$  and  $l_5$ . Since  $l_5 \in M$  whereas  $l_3$  is not,  $l_3$  would cause a higher penalty than  $l_5$  for the same level of degradation.
- If  $l \in M$  is not affected by the disaster, the LP may be recovered with degraded service with a new path and spectrum.  $l_2$  is an example of such an LP.
- If  $l \in U$  is not affected by the disaster, it may be recovered with degradation and re-assigned spectrum on the same path. An example of such an LP is  $l_1$ .

2) *Penalty Functions*: When the data rate of an LP is degraded, there is a penalty that is accrued due to violation of the SLA. In this paper, we assume that each LP brings revenue to the network and revenue is equal to the data rate of the LP. There are two different non-decreasing penalty functions - one for LPs within the mitigation zone and one for outside the mitigation zone.  $P_1(d)$  is used as the penalty function for the LPs inside the mitigation zone. Here, the degradation factor  $d$  is the percentage of the data rate degraded (the percentage of reduction in the LP's data rate). For the LPs outside the mitigation zone, we consider four different penalty functions,  $P_2(d)$ ,  $P_3(d)$ ,  $P_4(d)$  and  $P_5(d)$ , to explore the performance of our algorithm with respect to a variety of functions.  $P_2(d)$ ,  $P_3(d)$  and  $P_4(d)$  are used to represent sub-linear, linear and super-linear functions respectively, whereas  $P_5(d)$  represents the case when a LP loses all its revenue when its service is degraded by *any* amount. These penalty functions are given

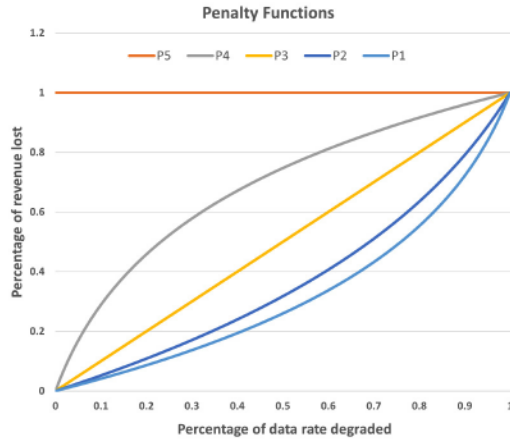


Fig. 2. Penalty functions.

by equations (1) to (5) and shown in Fig. 2.

$$P_1(d) = \frac{\log(1 - 0.9 \times d)}{\log(1 - 0.9 \times 1)} \quad (1)$$

$$P_2(d) = \frac{\log(1 - 0.8 \times d)}{\log(1 - 0.8 \times 1)} \quad (2)$$

$$P_3(d) = d \quad (3)$$

$$P_4(d) = \frac{\log(10 \times d + 1)}{\log(10 \times 1 + 1)} \quad (4)$$

$$P_5(d) = 1, \quad 0 < d \leq 1. \quad (5)$$

The penalty functions indicate the relationship between the degradation factor and the percentage of the revenue lost. The absolute value of the penalty is the value of the penalty function times the total revenue of the LP. For example, suppose the original data rate of an affected LP that is inside the mitigation zone is 100 Gbps but the LP is recovered with 75 Gbps. In this case, equation (1) is used and the value of the penalty function corresponding to 25% data rate degradation is 0.11. Therefore, the absolute penalty is  $0.11 \times 100 = 11$ . For the no degradation case, the value of the penalty function is 0, so there is no penalty at all. The value of the penalty function is 1 in the full degradation case (i.e., the LP is dropped). If an LP is blocked/dropped during the recovery or re-assignment, all the revenue is considered to be lost and the absolute penalty is equal to the revenue.

As shown in Fig. 2,  $P_1(d) < P_i(d)$ ,  $i = 2, 3, 4, 5$ , for a given degradation factor  $d$ . This setting is based on the intuition that users of services that are far away from the disaster zone (i.e.,  $l \in U$ ) do not want to be affected during the recovery process, and therefore there is a higher penalty when their service is degraded. The mitigation zone is designed as the “help zone” to solve the capacity bottleneck problem in the damaged network, so the LPs inside the mitigation zone are charged a lower penalty.

The objective of the disaster management problem is to recover the affected LPs and re-accommodate the unaffected LPs, while minimizing the total penalty. The re-accommodation of the unaffected LPs involves the adjustment of the pre-disaster assignment of LPs in the damaged network. The purpose of re-accommodation is to provide flexibility in

recovery, without which a large penalty would be incurred. By utilizing this flexibility appropriately, LPs can be recovered or re-assigned with a low total penalty.

This problem is extremely challenging as it involves finding a recovery path and spectrum for LPs and selecting the appropriate degradation factor for each LP. It is well known that even the spectrum assignment problem is NP-hard in mesh networks. In this work, we present an ILP and a heuristic algorithm to do the routing and spectrum assignment, and find the appropriate degradation factors.

#### IV. AN ILP FORMULATION

In this section, we formulate an ILP model to solve the problem. Here, we assume that the possible degradation factors are 0% to 100% with a step size of 10%. The parameters are presented as follows:

- $L'$ : the set of *recoverable* lightpaths
- $L^*$ : the set of unaffected lightpaths that lie outside the mitigation zone
- $J_l$ : the path index of LP  $l$  before the disaster happens
- $F$ : Set of FSs on a fiber
- $K$ : number of candidate paths for a lightpath
- $D_l$ : the original data rate of LP  $l$
- $\alpha_l^{k,d}$ : number of required FSs for LP  $l$  when it is assigned with the candidate path  $k$  and degradation factor  $10 \times d\%$ . The highest possible modulation format is used. These values are generated offline.

The variables are as follows:

- $\beta_l^s$ : Boolean variable that equals 1 if FS index  $s$  is used in the recovered or re-assigned LP  $l$ , and 0 otherwise
- $J_l^k$ : Boolean variable that equals 1 if LP  $l$  is recovered or re-assigned with candidate path  $k$ , and 0 otherwise
- $A_l$ : Boolean variable that equals 1 if LP  $l$  is recovered or re-assigned, and 0 otherwise
- $\theta_l^d$ : Boolean variable that equals 1 if LP  $l$  is recovered or re-assigned with  $10 \times d\%$  degradation factor, and 0 otherwise
- $I_l^{k,d}$ : Boolean variable that equals 1 if LP  $l$  is recovered or re-assigned with candidate path  $k$  and degradation factor  $10 \times d\%$ , and 0 otherwise
- $f_s^l$ : the start FS index of LP  $l$  after recovery
- $f_e^l$ : the end FS index of LP  $l$  after recovery

Objective: *Minimize*

$$\sum_{l \in L'} D_l \times P_i \left( \sum_{d \in [0, 9]} d/10 \times \theta_l^d \right) + (1 - A_l) \times D_l. \quad (6)$$

where  $P_i(\cdot)$  is penalty function  $i$ .

The objective of the ILP is to minimize the total absolute value of the penalty after recovery. The absolute value of the penalty is the value of the penalty function times the total revenue of the LP (in this work the revenue of LP equals to LP's data rate).

The *constraints* are as follows:

$$\sum_{k \in [1, K]} J_l^k = A_l, \forall l \in L'. \quad (7)$$

Eq. (7) ensures that exactly one candidate path is selected for recovery if the LP is not selected to be dropped. The candidate paths are generated offline with a  $k$ -shortest-paths algorithm.

$$\sum_{d \in [0,9]} \theta_l^d = A_l, \forall l \in L'. \quad (8)$$

Eq. (8) ensures that one degradation option is selected if the LP is not selected to be dropped.

$$\sum_{s \in F} \beta_l^s = f_e^l - f_s^l, \forall l \in L'. \quad (9)$$

$$\sum_{d \in [0,9]} \sum_{k \in [1,K]} I_l^{k,d} \times \alpha_l^{k,d} = f_e^l - f_s^l, \forall l \in L'. \quad (10)$$

$$(|F| - s) \times \beta_l^s \geq 1 - f_s^l, \forall s \in F, \forall l \in L'. \quad (11)$$

$$s \times \beta_l^s \leq f_e^l, \forall s \in F, \forall l \in L'. \quad (12)$$

Eqs. (9) to (12) ensure that each LP is assigned enough FSs with spectrum contiguity. In Eq. (11),  $|F|$  is the number of slots on each fiber and  $s$  represents an arbitrary fixed frequency slot.

$$k \times J_l^k = J_l, \forall l \in L^*. \quad (13)$$

Eq. (13) ensures the paths of unaffected LPs that lie outside the mitigation zone are the same as before the disaster.

$$\sum_{l \in L'} \beta_l^s \leq 1, \forall e \in E, s \in F. \quad (14)$$

Eq. (14) ensures that LPs do not share FSs on a link.

$$J_l^k + \theta_l^d + A_l \geq 3 \times I_l^{k,d}, \forall s \in F, \forall l \in L', k = 1, 2, \dots, K. \quad (15)$$

$$J_l^k + \theta_l^d + A_l \leq I_l^{k,d} + 3, \forall s \in F, \forall l \in L', k = 1, 2, \dots, K. \quad (16)$$

Eq. (15) and (16) ensure that  $I_l^{k,d}$  equals 1 when  $J_l^k$ ,  $\theta_l^d$  and  $A_l$  are equal to 1.

While the ILP is useful for benchmarking on small problem instances, it is time-prohibitive for realistic problem sizes. Accordingly, we develop and present our heuristic algorithm for disaster recovery next.

## V. THE DRAMA+ ALGORITHM

In this section, the DRAMA+ algorithm is presented. DRAMA+ first determines the recovery order of LPs, and then proceeds to perform routing and spectrum assignment (RSA) with degradation factor selection for each LP.

### A. Order of Recovery

First, all the LPs except unrecoverable ones are sorted in terms of Initial Penalty (IP) in non-increasing order. The IP is defined as the penalty of a one-FS degradation if the LP is routed on the potential path. If the LP is inside the mitigation zone or affected by the disaster, the potential path is the shortest-longest-segment-path among the  $K$  shortest paths. The shortest-longest-segment-path is obtained by looking at the longest segment (subpath between 3R-regenerators) on each

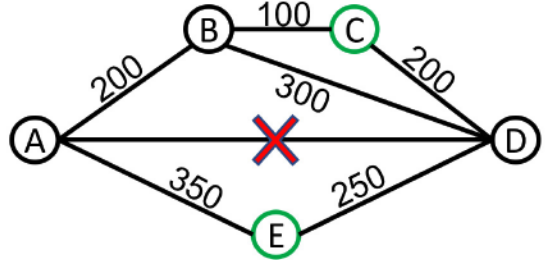


Fig. 3. An example to illustrate the potential path for IP calculation.

path and selecting the path with the shortest of these longest segments. The reason why we use shortest-longest-segment-path here is that, the modulation of a LP is determined by the longest transparent transmission segment. The path with the shortest-longest segment has the highest modulation format.

If the LP is outside the mitigation zone and not affected by the disaster, the potential path is the same as the original path before the disaster, since the route cannot be changed in this case based on our assumption. We emphasize that the potential path is only used to calculate the value of IP and it may not be the final routing of the LP.

An example for calculating the IP is shown in Fig. 3. Suppose there are 5 nodes in the network with two 3R-regenerators at nodes C and E. Suppose there is a LP from A to D and the original path is A-D, which is failed due to the disaster. There are three possible recovery paths here: A-B-C-D, A-B-D and A-E-D. Path A-B-C-D is cut into two segments (A-B-C and C-D) by the 3R-regenerator at node C. Thus the physical length of the longest segment of this path is 300 (A-B-C,  $200 + 100 = 300$ ). For path A-B-D, there is no 3R-regenerator, so the longest segment is the entire path and the physical length is 500. For the path A-E-D, the physical length of the longest segment is 350. Therefore, path A-B-C-D will be selected as the recovery path because it has the shortest-longest segment.

After the path is selected, the modulation format is determined by the physical length of the longest segment on this path. In this example, suppose the original data rate of the LP is 400 Gbps and 16QAM (each FS supports 50 Gbps for 16QAM) is selected as the modulation, then the number of FSs in the no-degradation case is 8. Therefore, the penalty of a one-slot degradation is the absolute penalty when the LP is recovered with 7 FSs. If this LP is inside the mitigation zone, then the degradation factor is 0.125 and  $P_1(0.125) = 0.052$ . The IP of this LP is  $400 \times 0.052 = 20.8$ . If the LP is outside the mitigation zone and affected by the disaster, then the IP is calculated with one of the penalty functions  $P_2(\cdot)$  to  $P_5(\cdot)$ . The reason behind sorting LPs in non-increasing order of IP is that LPs with large IPs will incur a higher penalty if they are not recovered, which is more likely to happen for LPs recovered down the order because resources have been already assigned to LPs up the order.

### B. Recovery Algorithm

We now describe the recovery algorithm. The pseudocode of DRAMA+ is shown in Algorithm 1.

**Algorithm 1** DRAMA+ Algorithm

---

**Input:**  $G(N, E)$ ,  $L$ ,  $D(C_d, R_d)$ ,  $M(C_m, R_m)$   
**Output:** Recovery of network

- 1: Initialize an empty LP set  $L'$
- 2: **for** each  $l \in L$  **do**
- 3:   **if**  $l \in D$  (i.e.,  $l$  is unrecoverable) **then**
- 4:     Release the spectrum of  $l$
- 5:   **else**
- 6:     add  $l$  to  $L'$
- 7:   **end if**
- 8: **end for**
- 9: Sort all  $l \in L'$  in terms of IP in non-increasing order
- 10: **for** Each LP  $l(s, d, w) \in L'$  **do**
- 11:   **if**  $l \in M$  or  $l$  is affected by disaster **then**
- 12:     Calculate a new path for  $l$  by CR algorithm
- 13:   **else**
- 14:     Maintain the original path
- 15:   **end if**
- 16:   Determine the modulation format and number of FSs
- 17:   **for** Each possible degradation option **do**
- 18:     Calculate  $PP = CP + FP$
- 19:   **end for**
- 20:   Select the degradation option that has the lowest PP
- 21:   Assign  $l$  with selected path (segments) and spectrum with First Fit with selected degradation; block  $l$  if FSs not available
- 22: **end for**

---

In lines 1-8, the spectrum that was assigned to unrecoverable LPs is released, and the recoverable LPs are added to set  $L'$ . In line 9, LPs in  $L'$  are sorted in terms of IP in non-increasing order.

From lines 10 to 22, for each LP in  $L'$ , we do RSA with the selection of degradation. The route of the LP is determined from lines 11 to 15. If the LP is affected by the disaster and outside the mitigation zone, the original path before the disaster is used without re-routing. In line 12, for a LP that is affected or inside the mitigation zone, we use an updated version of the Cost-Routing algorithm (CR) proposed in our previous paper [7] for the route. The current CR algorithm is proposed with dynamic spectrum consideration, whereas the algorithm in [7] is a static algorithm and cannot make routing decision based on different spectrum assignments. In the CR algorithm, we use the  $K$  shortest paths as the candidate paths and select the path with the lowest cost, where the cost of a path is defined as follows:

$$Cost = H \times M \times \frac{\nu_{bd}}{\nu_{ls}}, \quad (17)$$

where  $H$  denotes the number of hops and  $M$  denotes the modulation factor of the path. The modulation factor is determined by the longest segment of the path and the highest possible modulation format is selected. For BPSK, QPSK, 8QAM and 16QAM, the corresponding spectrum efficiencies are 1, 2, 3 and  $4 \times 12.5$ Gbps/Hz; Therefore we choose the corresponding modulation factor as 1, 0.5, 0.34 and 0.25, respectively.  $\nu_{bd}$  denotes the number of FSs needed without degradation,

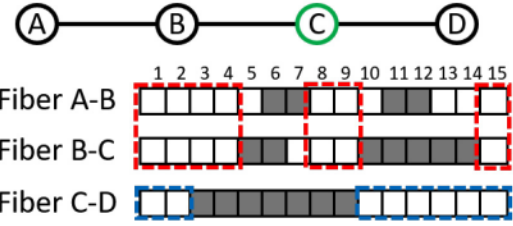


Fig. 4. An example of longest-spectrum segment.

which is determined by the data rate and modulation format.  $\nu_{ls}$  denotes the longest-spectrum segment of the path in terms of FSs. An example of the calculation of  $\nu_{ls}$  is shown in Fig. 4.

Consider the path A-B-C-D in the example in Fig. 3. The spectrum usage is shown in Fig. 4. Based on spectrum continuity and spectrum contiguity, there are 3 available spectrum segments on fiber A-B and B-C (marked in red). On link C-D, there are two spectrum segments (marked in blue). Since the 3R-regenerator is able to realize spectrum conversion, the longest-spectrum segment of this path is 4 slots. The longest-spectrum segment indicates the number of slots in the largest contiguous set of FSs that can be carried on this path. The variable  $\nu_{ls}$  is used in the CR algorithm for the purpose of load balance. The value of  $\nu_{ls}$  is lower if more FSs on this path are used, which causes the cost to be higher. If  $\nu_{ls} = 0$ , then we set the cost of the path to  $\infty$ . If the cost of all the paths is  $\infty$ , the LP is blocked.

From lines 16 to 20, the appropriate degradation factor is selected. After the path is selected, the modulation format is determined by the physical length of the longest segment, and the number of FSs needed without service degradation is calculated. For each candidate degradation option, we calculate the Potential Penalty (PP), which is defined as the sum of the Current Penalty (CP) and Future Penalty (FP), as explained below. The candidate option with the lowest PP is selected for the LP. For instance, suppose there is a 100 Gbps LP assigned with QPSK; the number of slots needed without degradation is 4. Then, we calculate the PP for 5 degradation options (0 to 4 slots, respectively) and select the lowest case. It is possible that the number of slots needed without degradation is 4 but the longest-spectrum segment on this path is 2. In this scenario, the degradation is selected from 3 options (0 to 2 slots).

When an LP is considered for degradation, spectrum can be saved with a high degradation factor; however, the current LP will be charged with a larger penalty. Therefore, balancing the tradeoff between current penalty and future spectrum saving or future penalty is necessary. CP and FP are defined as follows.

CP is calculated based on the current degradation option with the penalty function. For instance, if a lightpath (400Gbps, 16QAM, 8 slots without degradation, same as the example in Fig. 3), inside the mitigation zone is assigned with 7 slots, then the CP is 20.8.

FP is calculated based on the consequence if the LP is assigned with a degradation option:

$$FP = \frac{\nu'}{\nu_{ls}} \times \lambda, \quad (18)$$

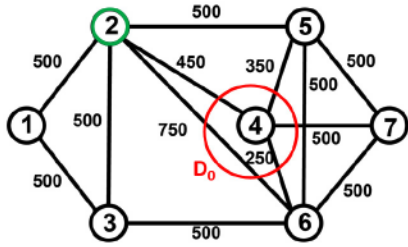
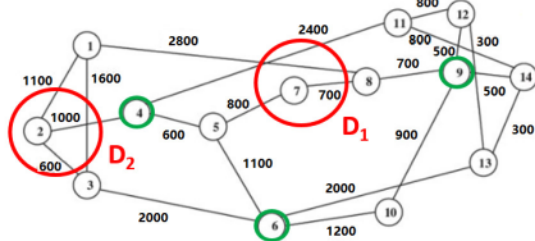


Fig. 5. 7-node small network.

Fig. 6. 14-node NSF network.  $D_1$  and  $D_2$  are two disaster zones, and green circles are 3R-regenerator locations.

where  $\nu'$  is the number of slots needed for the degradation option, and  $\nu_{ls}$  is the longest-spectrum segment (as in Eq. (17)).  $\lambda$  represents the remaining data rate on the path of the current LP, which is equal to the number of available slots times the data rate per FS of the highest possible modulation format on the path.  $\lambda$  is used to evaluate the loss of spectrum of the current assignment and degradation, which can be used by future LPs.  $\nu'/\nu_{ls}$  is used to evaluate the cost of fragmentation.

Finally, in line 21, the LP is assigned with selected path and degradation with first fit (FF) spectrum assignment. The time complexity of routing part is  $O(K \cdot |N| \cdot |F|)$ , as the number of hops in a path is  $O(|N|)$ . For the degradation selection part, the time complexity is  $O(|N| \cdot |F|)$ . Therefore, for the recovery or reassignment of each LP, the time complexity of DRAMA+ is  $O(K \cdot |N| \cdot |F|)$ .

## VI. SIMULATION RESULTS

### A. Simulation Setting

We now present performance results for both ILP and DRAMA+. A small network (SN) with 7 nodes and 13 links, shown in Fig. 5, is used for ILP testing. The link lengths in kilometers are shown next to the links. The number of FSs available on each fiber is assumed to be 100.

The network topologies used for evaluating DRAMA+ are the NSF network (14 nodes and 22 links, shown in Fig. 6) and the COST239 network (11 nodes and 26 links, shown in Fig. 7). The number of FSs available on each fiber is assumed to be 352.

Four different given disasters are tested, besides random disaster scenarios. The given disasters are shown as red circles in Figs. 5, 6, and 7. These given disasters are representative of disasters at the center of the network ( $D_0$  and  $D_1$ ), and near the edge of the network ( $D_2$  and  $D_3$ ), and our aim is to evaluate

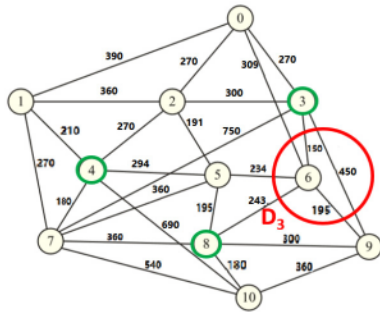
Fig. 7. 11-node COST239 network.  $D_3$  is a disaster zone, and green circles are 3R-regenerator locations.

TABLE I  
REQUIRED FSs AND DISTANCE LIMITATIONS [3]

Modulation	Data Rate		
	40	100	400
16QAM (500 km, 12.5 Gbps)	2	3	9
8QAM (1000 km, 25 Gbps)	3	4	12
QPSK (2000 km, 37.5 Gbps)	4	5	17
BPSK (>2000 km, 50 Gbps)	5	9	33

the performance for these special cases which cause different levels of bottlenecks. We assume that all the nodes and links inside the disaster zone are disabled by the disaster. For instance, for disaster zone  $D_1$ , node 7 and links 1-8, 5-7, 7-8, and 4-11 are disabled. A set of unidirectional LPs is generated before the disaster happens. The source node and destination node are uniformly randomly selected. The required data rate of the traffic is generated from the following distribution: 40 Gbps, 100 Gbps, and 400 Gbps with probability 0.2, 0.5, and 0.3, respectively. We assume that four modulation formats are used: 16-QAM, 8-QAM, QPSK, and BPSK. The transparent physical distance limitations are shown in parentheses in Table I for each modulation format.<sup>2</sup> The number of required FSs without degradation is determined by its data rate and selected modulation format. The number of FSs corresponding to different data rates and different modulation formats are also shown in Table I.

The required numbers of FSs of a lightpath for a given modulation format is calculated as follows:

$$F = \left\lceil \frac{w}{\eta_m} \right\rceil \quad (19)$$

where  $w$  is the data rate of the lightpath,  $\eta_m$  is the spectrum efficiency of modulation format  $m$  (defined as data rate per FS, shown in Table I after each modulation format) used for the lightpath. In DRAMA+ simulation, 1000 LPs are generated before the disaster happens, whereas 200 LPs are generated for the ILP. These LPs are assigned the shortest-longest-segment path among  $K$ -shortest paths ( $K = 5$ ) and spectrum using FF assignment. An LP is not established if the selected path does not have available slots.

We assume that the locations of 3R-regenerators are given in the translucent network. In the 7-node SN, we assume that a

<sup>2</sup>We assume that there is no physical distance limitation for BPSK.

3R-regenerator is placed at node 2. For the two large networks, all the nodes in the network are sorted using the betweenness Centrality (BC), which is defined as follows:

$$BC_i = \frac{2}{(n-1)(n-2)} \times \sum_{s \neq i \neq d} \frac{\sigma_{sd}(i)}{\sigma_{sd}} \quad (20)$$

where  $BC_i$  is the betweenness centrality of node  $i$ ,  $n$  is the total number of nodes in the network,  $\sigma_{sd}(i)$  is the number of the shortest paths (in number of hops) from  $s$  to  $d$  that cross node  $i$ ,  $\sigma_{sd}$  is the number of shortest paths from  $s$  to  $d$  (shortest paths have the same number of hops). In NSF network and COST network, we assume that there are three 3R-regenerators placed on the nodes that have the highest  $BC$  ( $BC$ -based placement).  $BC$  represents the degree of interaction between a node and other nodes so we use  $BC$  to place the 3R-regenerators. This test setting is designed to show the performance of the proposed algorithm when the 3R-regenerators are placed at good locations, though we have to emphasize that optimizing 3R-regenerator locations is not a goal of this paper. 3R-regenerator node locations are shown in green in Fig. 5, Fig. 6, and Fig. 7. We also test the performance for random 3R-regenerator placement (RP), where three 3R-regenerators are uniformly randomly placed. In the ILP testing, we assume that there is one 3R-regenerator placed at node 2 in SN.

In the simulation, for the  $BC$ -based 3R-regenerator placement, 50 different LP sets are generated for each experiment, and 95% confidence intervals are plotted. For RP, 10 different placements are randomly generated, and for each placement, 10 different LP sets are generated. The average over these 100 different placement-LP set pairs is plotted with 95% confidence interval. In ILP, 10 different LP sets are used for testing.

We compare the ILP and DRAMA+ with the following baseline cases:

- DRAMA+ algorithm with no degradation (DRAMA+ND). During the recovery, the lightpaths are routed using the path selection part in DRAMA+, while the degradation is set as no degradation without the calculations of current penalty and future penalty. This baseline algorithm is designed to show the effectiveness of the degradation selection in DRAMA+.
- DRAMA+ with shortest-longest-segment path (DRAMA+SLS). During the recovery, the lightpaths are routed by the shortest-longest-segment path among the  $K$  shortest paths in the damaged network, while the degradation is determined by the degradation selection part in DRAMA+ algorithm. This baseline algorithm is designed to show the effectiveness of CR path selection in DRAMA+.
- Shortest path and first fit (SPFF). The lightpath is recovered by using the shortest path (in number of hops) and FF spectrum assignment without degradation.

The performance of ILP and heuristic algorithms are evaluated in terms of total penalty and blocking ratio. The total penalty is the sum of penalties charged to all the recoverable

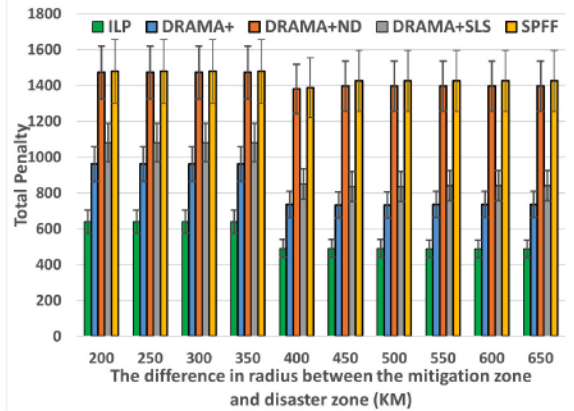


Fig. 8. Total penalty of recovery in SN.

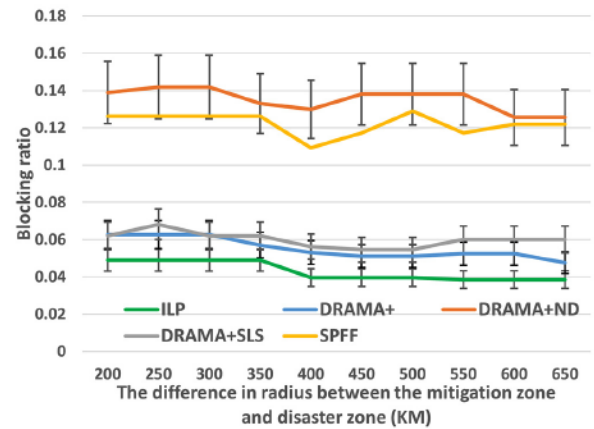


Fig. 9. Blocking performance of recovery in SN.

LPs due to degradation or blocking. In the total penalty evaluation of the heuristic algorithms, we also show the penalty before any recovery is initiated to help understand the benefits of recovery by the various algorithms in terms of reducing the penalty. The penalty before recovery is shown as a dashed line named BeforeRecovery. The blocking ratio is defined as the number of blocked recoverable LPs to the total number of recoverable LPs.

### B. ILP

Here we compare the results of ILP and DRAMA+ for SN for different mitigation zones. The penalty function  $P_1$  is used for LPs inside the mitigation zone and the penalty function  $P_2$  is used for LPs outside the mitigation zone.

As Figs. 8 and 9 show, the ILP produces the lowest penalty, but the performance of DRAMA+ is significantly better than the baseline algorithms. Both the total penalty of recovery and blocking ratio decrease as the mitigation zone increases, indicating that the flexibility of allowing degraded service recovery is helpful in improving the performance. The penalty of DRAMA+ is reduced by up to 50% over SPFF, while the penalty of ILP is up to 45% lower compared to that of DRAMA+. We can see that DRAMA-ND and SPFF have higher blocking ratios, because routing plays a more important role when the network is small. The modulation formats

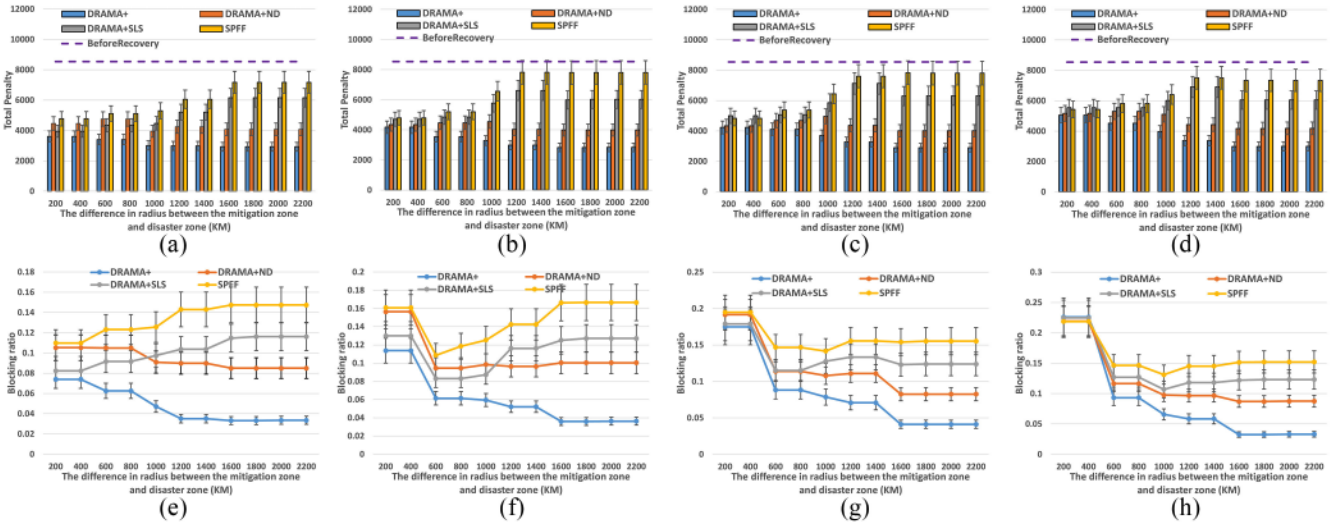


Fig. 10. Performance results for NSF network with BC-based 3R-regenerator placement for disaster zone  $D_1$ .

can be easily changed if the LP can be routed across 3R-regenerators since the physical length of the longest segment can be vastly decreased when the number of hops is small.

### C. DRAMA+

In the simulations, four different penalty function pairs are used. For the LPs inside the mitigation zone, the penalty function  $P_1$  is always used, while penalty functions  $P_2$ ,  $P_3$ ,  $P_4$  and  $P_5$  are separately used for the LPs outside the mitigation zone. The performance of DRAMA+ for BC-based 3R-regenerator placement are shown in Figs. 10 to 13 for disaster zones  $D_1$ ,  $D_2$ , and  $D_3$ .

As we can see from Fig. 10(a) to 10(d), DRAMA+ is better than all the baseline algorithms in terms of total penalty. Further, the total penalty for DRAMA+ decreases as the mitigation zone expands, which shows that DRAMA+ can take advantage of the additional flexibility due to a larger mitigation zone. For example, when the size of the mitigation zone (characterized by the difference in radius between the disaster and mitigation zone circles) is 2000 km, we see that the penalty of DRAMA+ is reduced by 59%, 63%, 62% and 59% over SPFF for the four different penalty functions outside the mitigation zone, respectively. We also observe that DRAMA+ND and DRAMA+SLS are better than SPFF. When the size of the mitigation zone is 2000 km and penalty functions  $P_1$  and  $P_2$  are used, the penalties of DRAMA+ND and DRAMA+SLS are reduced by 43% and 14% respectively. This observation shows that DRAMA+ can provide a better recovery than SPFF even when only one of path selection or degradation selection is used. In this case (2000 km mitigation zone with  $P_1$  and  $P_2$ ), we also see that DRAMA+, DRAMA+ND and DRAMA+SLS reduce the penalty from BeforeRecovery by 65%, 52%, and 27%, respectively.

The blocking ratio for disaster zone  $D_1$  in the NSF network is shown in Fig. 10(e) to 10(h). Even though the objective of DRAMA+ is to minimize the total penalty, we see that it performs the best in terms of blocking ratio as well. We also note that the blocking ratio generally decreases with the

increase of the mitigation zone size for DRAMA+, which means the flexibility gained from mitigation zone is fully utilized during recovery. Interestingly, the penalties of baseline algorithms *increase* as the size of the mitigation zone increases. This suggests that even though the larger mitigation zone provides a higher flexibility during recovery, the risk and cost of inappropriate LP re-assignment is also higher. During the re-assignment, if the degree of degradation is relatively high, even if we are saving spectrum, the penalty could be higher because of this high degradation. Meanwhile, if the degree of degradation is low, the penalty could also be high because of high blocking ratio of other connections. Therefore, using a judicious strategy to take advantage of this flexibility is necessary.

In Fig. 11, we show the blocking ratios of DRAMA+ in detail for disaster zone  $D_1$  with the four penalty function pairs. DRAMA+iM and DRAMA+oM are the blocking ratios of the recoverable LPs inside and outside the mitigation zone, respectively. DRAMA+oMU is the blocking ratio of LPs outside the mitigation zone that are not affected by the disaster. We can see that when the size of mitigation zone is large, the blocking ratios of LPs outside the mitigation zone are lower than the blocking ratios of LPs inside the mitigation zone, and the blocking ratios of unaffected LPs outside the mitigation zone are much lower and even drop to 0. This result satisfies the motivation for DRAMA+, i.e., traffic far away from the disaster is less affected.

In NSF network, for disaster zone  $D_2$  with BC-based 3R-regenerator placement, the performance of DRAMA+ is again better than baseline algorithms (shown in Fig. 12). As we can see, DRAMA+ is able to provide a better recovery for every penalty function pair case. For example, when the size of mitigation zone is 3400 km, the penalty of DRAMA+ is reduced by 37%, 30%, 25% and 39% over SPFF, and 44%, 50%, 48% and 53% over BeforeRecovery for the four pairs of penalty functions, respectively.

We also note that DRAMA+ND is better than DRAMA+SLS for disaster zone  $D_1$ , whereas the penalty of DRAMA+SLS is lower than DRAMA+ND in disaster zone

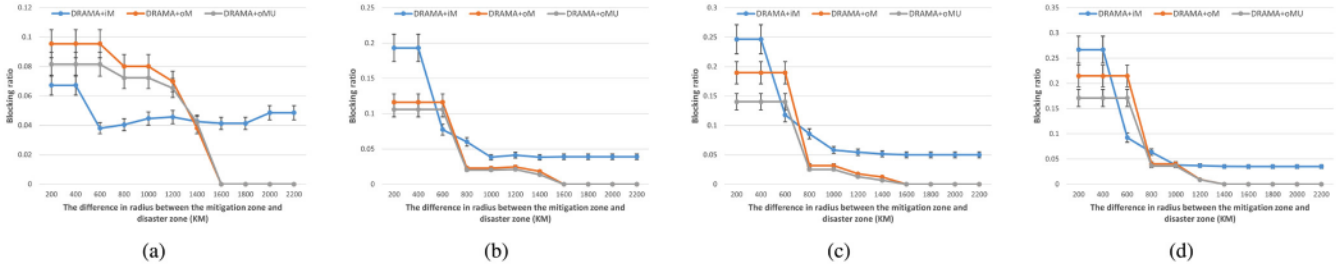


Fig. 11. Breakdown of blocking ratios for LPs in NSF network for disaster zone  $D_1$  with various penalty function pairs: (a)  $P_1$ - $P_2$ , (b)  $P_1$ - $P_3$ , (c)  $P_1$ - $P_4$ , (d)  $P_1$ - $P_5$ .

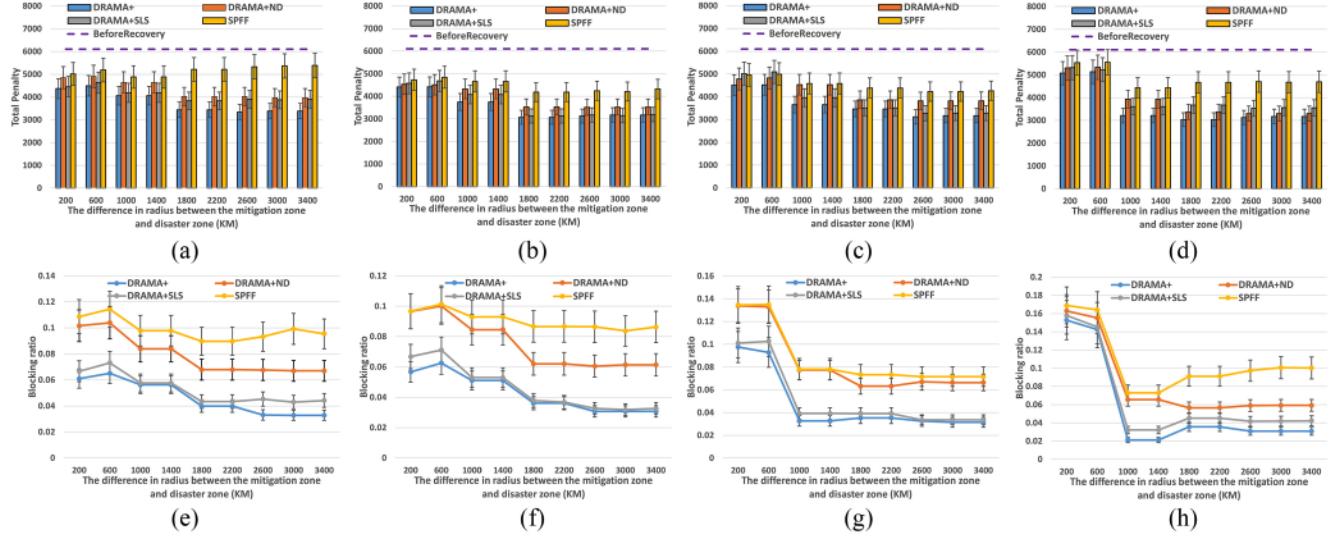


Fig. 12. Performance results for NSF network with BC-based 3R-regenerator placement for disaster zone  $D_2$ .

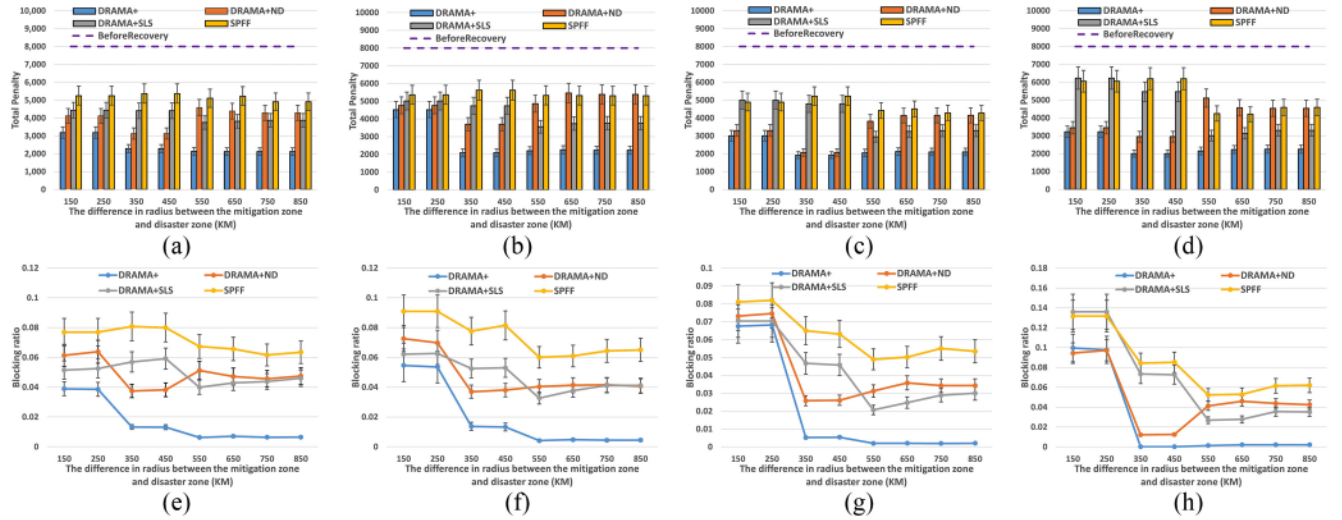


Fig. 13. Performance results for translucent COST239 network with BC-based 3R-regenerator placement for disaster zone  $D_3$ .

$D_2$  case. The reason is that for disaster zone  $D_1$ , the damaged part of the network creates a bottleneck around node 7, which leads to fewer options for path selection during recovery, especially for many LPs routed from one side of the network to the other before the disaster happens (e.g., from node 1 to 13 or from node 12 to 3). If the bottleneck problem created by the disaster is not so severe (such as for disaster zone

$D_2$ , DRAMA+SLS is better than DRAMA+ND, as shown in Fig. 12. In both cases, DRAMA+ is better than all the baseline algorithms.

In COST239 network, for disaster zone  $D_3$  with BC-based 3R-regenerator placement, the total penalty of DRAMA+ is much lower than baseline algorithms (shown in Fig. 13). When the size of mitigation zone is 850 km, the penalty of

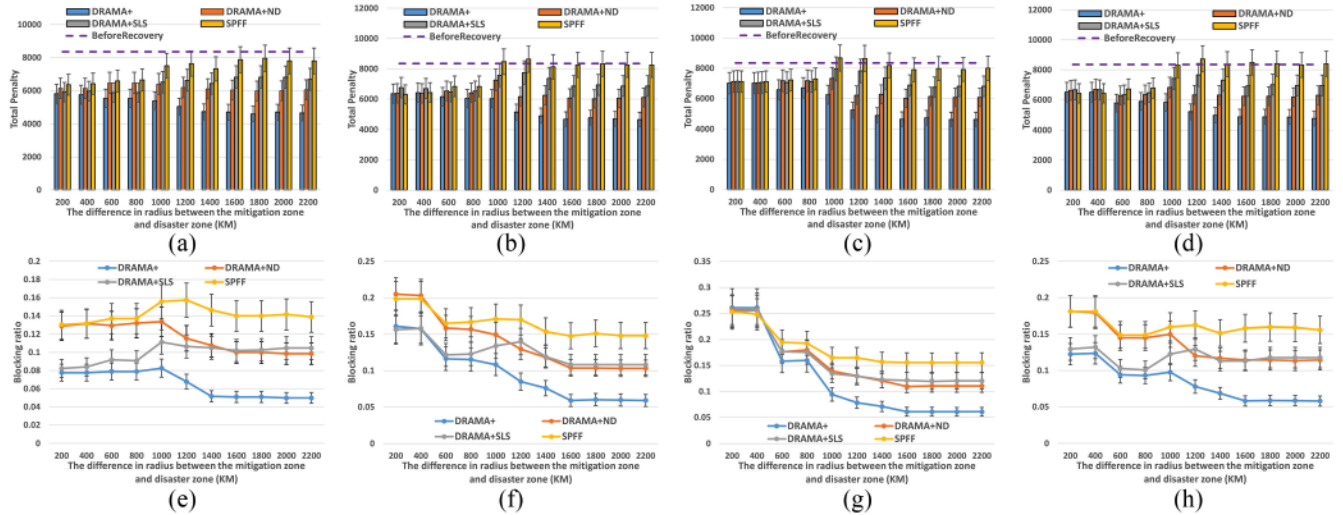


Fig. 14. Performance results for NSF network with random 3R-regenerator placement for disaster zone  $D_1$ .

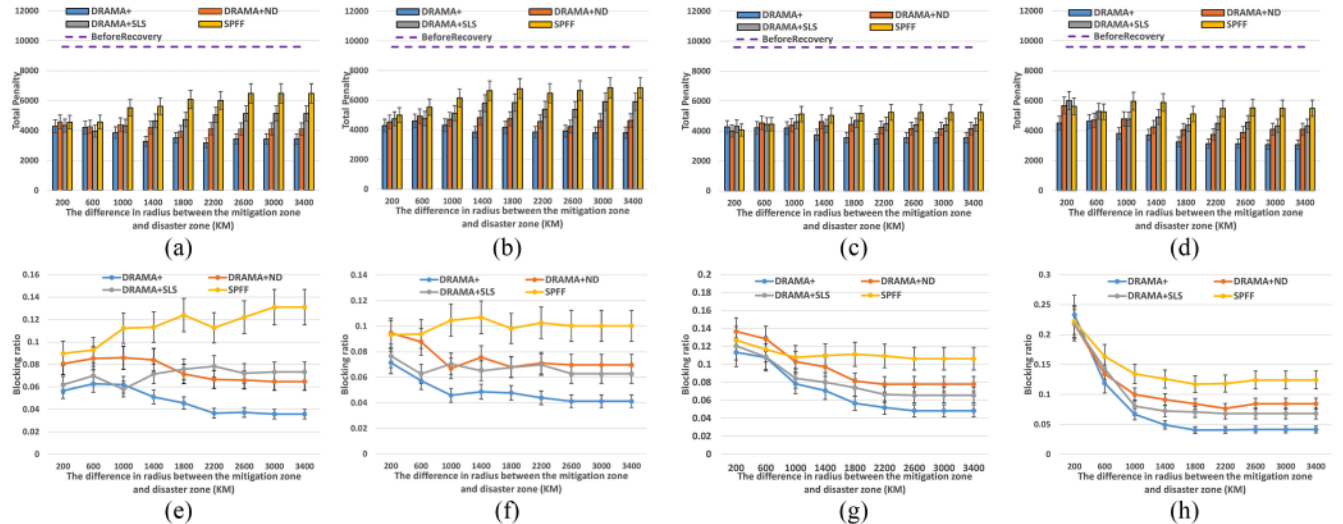


Fig. 15. Performance results for NSF network with BC-based 3R-regenerator placement when the disasters are randomly selected.

DRAMA+ is reduced by 56%, 58%, 50% and 50% over SPFF for the four different pairs of penalty functions, respectively. The blocking ratios of DRAMA+ are also much lower than those of baseline algorithms. Especially in large mitigation zone cases, the blocking ratios of DRAMA+ are very close to 0. Moreover, because of the smaller physical size of COST239, it is easier to recover traffic in this network, which means higher level modulations and fewer FSs are used for the LPs. Therefore, more LPs can be assigned to the COST239 before disaster happens and more LPs are affected after disaster. Therefore the penalty without recovery (BeforeRecovery) is very high. This is the reason why the gap between DRAMA+ and BeforeRecovery is much larger compared to cases in the NSF network. We can see that when the size of the mitigation zone is 850 km, the total penalty of DRAMA+ is reduced by 89%, 88%, 91%, and 88% over BeforeRecovery with the four penalty functions pairs.

We see from Fig. 14 that DRAMA+ also outperforms baseline algorithms when the 3R-regenerators are placed randomly in the NSF network. These results show that DRAMA+ is

able to effectively recover the LPs by considering the locations of the 3R-regenerators. Comparing the performance for the two different 3R-regenerator placement schemes, when the size of the mitigation zone is 2000 km, the penalty of DRAMA+ with BC-based 3R-regenerator placement (shown in Fig. 10) is reduced by 40%, 43%, 43%, and 42% over DRAMA+ with random 3R-regenerator placement for the four different pairs of penalty functions, respectively. Also, the penalty of DRAMA+ is reduced by 44%, 42%, 44%, and 45% over BeforeRecovery for the four different pairs of penalty functions.

While the previous results showed the recovery performance of DRAMA+ in specific disaster scenarios, we now present results for random disasters in Fig. 15. Here, the centers of disasters are uniformly randomly selected from all the nodes, while the sizes of the disasters are uniformly distributed in the range [100, 400] km. 10 different disasters are generated and 10 different LP sets (1000 LPs in each set) are used for each disaster. We can see that DRAMA+ has a better performance in both total penalty and blocking ratio. For example, when the

size of mitigation zone is 3400 km, the penalty of DRAMA+ is reduced by 47%, 44%, 32%, and 44% over SFPP, and 64%, 60%, 63%, and 68% over BeforeRecovery for the four penalty function pairs, respectively.

## VII. CONCLUSION

Disaster management is an important issue in elastic optical networks. The recovery performance can be enhanced by allowing the network to recover services at a degraded level as opposed to a fully-recover-or-drop approach. In this paper, we proposed the concept of mitigation zone to provide the network operator flexibility in re-assigning network resources, and formulated the recovery problem as one of minimizing the penalty due to dropped or degraded lightpaths. An ILP was formulated and a heuristic algorithm called DRAMA+ was developed. We compared the performance of DRAMA+ with several baseline algorithms. The results show that DRAMA+ performs better in terms of total penalty and blocking ratio in several scenarios.

## REFERENCES

- [1] M. Jinno, H. Takara, B. Kozicki, Y. Tsukishima, Y. Sone, and S. Matsuoka, "Spectrum-efficient and scalable elastic optical path network: Architecture, benefits, and enabling technologies," *IEEE Commun. Mag.*, vol. 47, no. 11, pp. 66–73, Nov. 2009.
- [2] Y. Hirota, H. Tode, and K. Murakami, "Multi-fiber based dynamic spectrum resource allocation for multi-domain elastic optical networks," in *Proc. 18th OptoElectron. Commun. Conf. Held Jointly Int. Conf. Photon. Switching (OECC/PS)*, Jun. 2013, pp. 1–2.
- [3] C. Wang, G. Shen, and S. K. Bose, "Distance adaptive dynamic routing and spectrum allocation in elastic optical networks with shared backup path protection," *J. Lightw. Technol.*, vol. 33, no. 14, pp. 2955–2964, Jul. 15, 2015.
- [4] J. Wu, M. Xu, S. Subramaniam, and H. Hasegawa, "Routing, fiber, band, and spectrum assignment (RFBSA) for multi-granular elastic optical networks," in *Proc. IEEE Int. Conf. Commun. (ICC)*, May 2017, pp. 1–6.
- [5] J. Wu, M. Xu, S. Subramaniam, and H. Hasegawa, "Joint banding-node placement and resource allocation for multi-granular elastic optical networks," in *Proc. IEEE Global Commun. Conf.*, Dec. 2017, pp. 1–6.
- [6] R. Zou, S. Subramaniam, H. Hasegawa, and M. Jinno, "P-cycle design for translucent elastic optical networks," in *Proc. IEEE Global Commun. Conf.*, Dec. 2019, pp. 1–6.
- [7] R. Zou, H. Hasegawa, M. Jinno, and S. Subramaniam, "Link-protection and FIPP p-cycle designs in translucent elastic optical networks," *J. Opt. Commun. Netw.*, vol. 12, no. 7, pp. 163–176, Jul. 2020.
- [8] B. Ramamurthy, H. Feng, D. Datta, J. P. Heritage, and B. Mukherjee, "Transparent vs. opaque vs. translucent wavelength-routed optical networks," in *Proc. OFC/IOOC*, vol. 1, 1999, pp. 59–61.
- [9] G. Shen, H. Guo, and S. Bose, "Survivable elastic optical networks: Survey and perspective," *Photon. Netw. Commun.*, vol. 31, no. 1, pp. 71–87, 2016.
- [10] R. Zou and S. Subramaniam, "Novel P-cycle selection algorithms for elastic optical networks," in *Proc. Int. Conf. Opt. Netw. Des. Model. (ONDM)*, May 2019, pp. 154–167.
- [11] R. Zou, H. Hasegawa, and S. Subramaniam, "DRAMA: Disaster management algorithm with mitigation awareness for elastic optical networks," in *Proc. 17th Int. Conf. Des. Rel. Commun. Netw. (DRCN)*, Apr. 2021, pp. 1–7.
- [12] H. Yu and C. Yang, "Partial network recovery to maximize traffic demand," *IEEE Commun. Lett.*, vol. 15, no. 12, pp. 1388–1390, Dec. 2011.
- [13] H. M. N. S. Oliveira and N. L. S. da Fonseca, "Algorithm for FIPP p-cycle path protection in flexgrid networks," in *Proc. IEEE Global Commun. Conf.*, 2014, pp. 1278–1283.
- [14] S. Li, R. Gu, G. Zhang, Y. Wang, Y. Wang, and Y. Ji, "Order aware service recovery algorithm in elastic optical network with multiple failures," in *Proc. Int. Conf. Netw. Netw. Appl. (NaNA)*, 2019, pp. 135–141.
- [15] M. W. Ashraf, S. M. Idrus, R. A. Butt, and F. Iqbal, "Post-disaster least loaded lightpath routing in elastic optical networks," *Int. J. Commun. Syst.*, vol. 32, no. 8, p. e3920, 2019.
- [16] M. Klinkowski and K. Walkowiak, "Offline RSA algorithms for elastic optical networks with dedicated path protection consideration," in *Proc. 4th Int. Congr. Ultra Modern Telecommun. Control Syst.*, 2012, pp. 670–676.
- [17] Y. Sone *et al.*, "Bandwidth squeezed restoration in spectrum-sliced elastic optical path networks (SLICE)," *IEEE/OSA J. Opt. Commun. Netw.*, vol. 3, no. 3, pp. 223–233, Mar. 2011.
- [18] Y. Wei, G. Shen, and S. K. Bose, "Span-restorable elastic optical networks under different spectrum conversion capabilities," *IEEE Trans. Rel.*, vol. 63, no. 2, pp. 401–411, Jun. 2014.
- [19] D. Zhou and S. Subramaniam, "Survivability in optical networks," *IEEE Netw.*, vol. 14, no. 6, pp. 16–23, Nov./Dec. 2000.
- [20] S. Ferdousi, F. Dikbiyik, M. Tornatore, and B. Mukherjee, "Joint progressive recovery of optical network and datacenters after large-scale disasters," in *Proc. Opt. Fiber Commun. Conf. Exhibit. (OFC)*, 2017, pp. 1–3.
- [21] C. Ma, J. Zhang, Y. Zhao, M. F. Habib, S. Savas, and B. Mukherjee, "Traveling repairman problem for optical network recovery to restore virtual networks after a disaster," *J. Opt. Commun. Netw.*, vol. 7, no. 11, pp. B81–B92, 2015.
- [22] M. Jinno, H. Takara, and Y. Sone, "Elastic optical path networking: Enhancing network capacity and disaster survivability toward 1 Tbps era," in *Proc. 16th Opto-Electron. Commun. Conf.*, 2011, pp. 401–404.
- [23] Y. Awaji, H. Furukawa, S. Xu, M. Shiraiwa, N. Wada, and T. Tsuritani, "Resilient optical network technologies for catastrophic disasters," *J. Opt. Commun. Netw.*, vol. 9, no. 6, pp. A280–A289, 2017.
- [24] Z. H. Nasralla, T. E. H. El-Gorashi, M. O. I. Musa, and J. M. H. Elmirghani, "Routing post-disaster traffic floods in optical core networks," in *Proc. Int. Conf. Opt. Netw. Des. Model. (ONDM)*, 2016, pp. 1–5.
- [25] P. N. Tran and H. Saito, "Enhancing physical network robustness against earthquake disasters with additional links," *J. Lightw. Technol.*, vol. 34, no. 22, pp. 5226–5238, Nov. 15, 2016.
- [26] F. Dikbiyik, M. Tornatore, and B. Mukherjee, "Minimizing the risk from disaster failures in optical backbone networks," *J. Lightw. Technol.*, vol. 32, no. 18, pp. 3175–3183, Sep. 15, 2014.
- [27] B. Mukherjee, M. F. Habib, and F. Dikbiyik, "Network adaptability from disaster disruptions and cascading failures," *IEEE Commun. Mag.*, vol. 52, no. 5, pp. 230–238, May 2014.
- [28] S. Huang, M. Xia, C. U. Martel, and B. Mukherjee, "A multistate multipath provisioning scheme for differentiated failures in telecom mesh networks," *J. Lightw. Technol.*, vol. 28, no. 11, pp. 1585–1596, Jun. 1, 2010.
- [29] R. Roy and B. Mukherjee, "Degraded-service-aware multipath provisioning in telecom mesh networks," in *Proc. Conf. Opt. Fiber Commun. Nat. Fiber Opt. Eng. Conf.*, 2008, pp. 1–3.



**Ruijia Zou** (Graduate Student Member, IEEE) received the B.S. degree in telecommunication engineering from Xidian University, Shaanxi, China, in 2017, and the M.S. degree in electrical and computer engineering from George Washington University, Washington, DC, USA, in 2019, where he is currently pursuing the Ph.D. degree in electrical engineering. His research interests include survivability design, disaster management in elastic optical network, and IoT.



**Hiroshi Hasegawa** (Senior Member, IEEE) received the B.E., M.E., and D.E. degrees in electrical and electronic engineering from the Tokyo Institute of Technology in 1995, 1997, and 2000, respectively. He is currently a Professor with the Graduate School of Engineering, Nagoya University, where he was an Associate Professor from 2005 to 2019. Before joining Nagoya University, he was an Assistant Professor with Tokyo Institute of Technology from 2000 to 2005. His current research interests include network/node architectures, devices, and design and control of photonic networks, multidimensional digital signal processing, and time-frequency analysis. He is a Senior Member of IEICE.



**Masahiko Jinno** (Fellow, IEEE) received the B.E. and M.E. degrees in electronics engineering from Kanazawa University, Ishikawa, Japan in 1984 and 1986, respectively, and the Ph.D. degree in engineering from Osaka University, Osaka, Japan, in 1995, for his work on ultra-fast optical signal processing based on nonlinear effects in optical fibers.

He currently serves as a Professor with the Faculty of Engineering and Design, Kagawa University, Takamatsu, Japan. Prior to joining Kagawa University in October 2012, he was a Senior

Research Engineer and a Supervisor with Nippon Telegraph and Telephone (NTT) Network Innovation Laboratories, NTT Corporation conducting pioneering research on spectrum- and energy-efficient elastic optical networks (EONs). From 1993 to 1994, he was a Guest Scientist with the National Institute of Standards and Technology, Boulder, CO, USA. He authored or coauthored over 200 peer-reviewed journal and conference papers in the fields of ultra-fast optical signal processing for high-capacity optical time division multiplexed transmission systems, optical sampling and optical time-domain reflectometry, ultra-wideband WDM transmission systems in the L-band and S-band, ROADM systems, GMPLS and application-aware optical networking, EONs, and spatial channel networks. His current research interests include architecture, design, management, and control of optical networks, optical transmission systems, optical cross-connects, optical switches, and rate- and format-flexible optical transponders.

Prof. Jinno received the Young Engineer's Award in 1993, the Best Tutorial Paper Awards in 2011 and 2021, the Best Paper Award in 2012, the Achievement Award in 2017, and the Milestone Certificate in 2017 from the Institute of Electronics, Information and Communication Engineers (IEICE), the Best Paper Awards from the 1997, 1998, 2007, and 2019 Optoelectronics and Communications Conferences, the Best Paper Award from the 2010 ITU-T Kaleidoscope Academic Conference, and the Outstanding Paper Award in 2013 from the IEEE Communications Society Asia-Pacific Board. He is a Fellow of IEICE and a Senior Member of Optica.



**Suresh Subramaniam** (Fellow, IEEE) received the Ph.D. degree in electrical engineering from the University of Washington, Seattle, in 1997.

He is a Professor of Electrical and Computer Engineering with the George Washington University, Washington, DC, where he directs the Lab for Intelligent Networking and Computing. He has published about 250 peer-reviewed papers in these areas. His research interests are in the architectural, algorithmic, and performance aspects of communication networks, with current emphasis on opti-

cal networks, cloud computing, data center networks, and IoT. He has received the five Best Paper Awards and the 2017 SEAS Distinguished Researcher Award from George Washington University. He has served in leadership positions for several top conferences, including IEEE ComSoc's flagship conferences of ICC, Globecom, and INFOCOM. He serves/has served on the editorial boards of seven journals, including the IEEE/ACM TRANSACTIONS ON NETWORKING and the IEEE/OPTICA JOURNAL OF OPTICAL COMMUNICATIONS AND NETWORKING. During 2012 and 2013, he served as the Elected Chair of the IEEE Communications Society Optical Networking Technical Committee. He is a Co-Editor of three books on Optical Networking. He was an IEEE Distinguished Lecturer from 2018 to 2021.